Marine CSEM in rough bathymetry

Daniil Shantsev, Lina Uri, Erlend Bjørdal, Martin Hansen, EMGS

SUMMARY

This abstract reviews the latest methods to optimize marine controlled-source electromagnetic (CSEM) data acquisition to ensure reliable interpretation in the presence of complex bathymetry. We specifically analyze how amplitude and phase of the recorded electric field are affected if the receiver is located at the slope within a seabed trench. The main trends observed on real data offshore Brazil can be reproduced by 3D forward modeling taking into account the precise bathymetry profile. Understanding these trends is very helpful for quality control (QC) and thus increases confidence in the acquired data. Applying error propagation analysis together with known accuracy of receiver positioning we can assess the limiting sensitivity of the CSEM data recorded within a trench with a given steepness.

INTRODUCTION

The marine CSEM method allows imaging of three-dimensional resistivity distribution in the subsurface. For the hydrocarbon exploration industry, this can be a very valuable tool, since oil and gas reservoirs are often more resistive than the surrounding sediments. It can also be useful to image other resistive structures such as salt and volcanic formations (Constable, 2010). The industry standard CSEM setup uses seabed receivers to record low-frequency electromagnetic (EM) fields that have been generated by a horizontal electric dipole source and propagated through the subsurface (Eidesmo et al., 2002). Placing receivers at the seabed is the best option to acquire deep-water (> 500 m) CSEM surveys because the EM field is strongly attenuated by the seawater.

The seafloor is usually much more resistive than the seawater. Therefore the seabed topography close to the receiver has a direct effect on the measured fields. In addition, the receiver frame and arms tend to be aligned with the seafloor; hence the measurements depend on the seafloor inclination at the exact receiver position. In the present paper we analyze how the bathymetry information manifests itself in the CSEM data. Such an analysis helps us optimize acquisition and data QC procedures in areas of rough bathymetry and eventually obtain a more accurate and reliable image of deep resistive structures.

DATA ACQUISITION

Figure 1 shows an example of the bathymetry profile along one of the source towlines during a multi-client CSEM survey offshore Brazil. The bathymetry in the area is very rough, and adequate spatial sampling can only be achieved by allowing receiver deployment in slopes or trenches. Several steep trenches go through the area from the shallow eastern part to the deeper western part. A typical example is shown in Figure 1: a 200 m deep trench with a maximal slope of ∼20 deg.

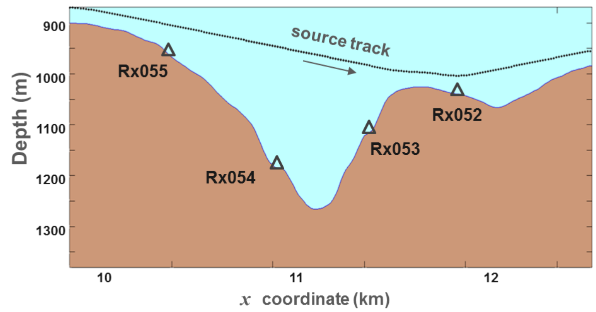

Figure 1: Seabed geometry, CSEM source trajectory and receiver positions (triangles) for a CSEM survey offshore Brazil.

The figure also shows the trajectory of the center of the 270 m long electric dipole source. In areas of flat bathymetry the source is usually towed at a constant elevation of 30 m above the seafloor. In this case, however, it is towed along a smooth path, avoiding the descent into the trench. A smooth trajectory of the source dipole is very beneficial since abrupt changes in the trajectory may reduce the accuracy of the source location, thus potentially compromising the quality of the CSEM data.

Accurate positioning of receivers is also necessary for any CSEM survey, but the presence of rough bathymetry magnifies this requirement. The seabed receiver positions have been measured acoustically using a USBL system. The coordinates of each receiver have been measured ∼100 times, from a number of different observation locations, allowing us to evaluate not only its position, but also the uncertainty in the position. Table 1 shows the standard deviation in the horizontal and vertical position for some receivers marked in Figure 1: it did not exceed 1.5 m for the given water depth of 1–1.4 km.

If a receiver is deployed on a slanted seafloor, there exists a possibility that it will slide down the slope *after* it has been positioned. In order to prevent such slides, all receivers in the present survey were equipped with steel spikes attached to the anchor. Furthermore, all receiver positions were also measured on recovery to verify that the receivers had not moved during the acquisition.

Table 1: Standard deviation in measured receiver positions.

Receiver	Depth [m]	Horizontal accuracy [m]	Vertical accuracy [m]
Rx052	1063.4	1.17	1.14
Rx053	1119.3	1.11	1.08
Rx054	1241.9	1.18	1.15
Rx080	1380.3	1.30	1.27

DOI http://dx.doi.org/10.1190/segam2013-1201.1

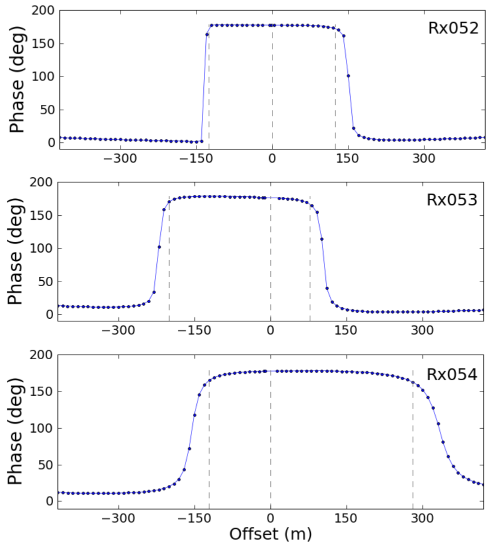

Figure 2: Short-offset PVO curves used for data QC for receivers marked in Figure 1. Receiver Rx052 on fairly flat seabed: symmetric PVO. Receivers Rx053 and Rx054 on the opposite slopes of a trench show asymmetric PVOs shifted towards the trench center. Frequency: 0.15 Hz.

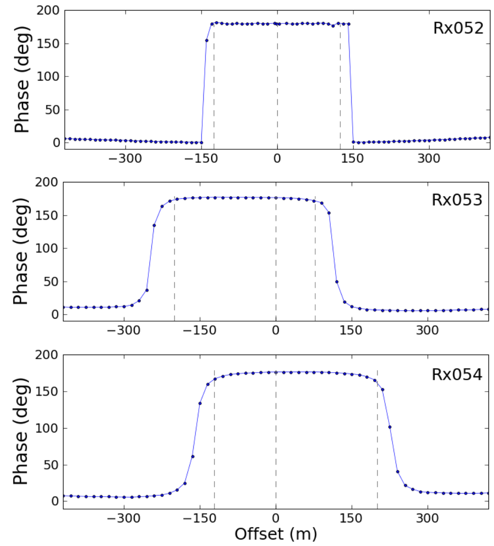

Figure 3: Synthetic PVO curves computed using bathymetry from the real survey for the same receivers as in Figure 2. Synthetic results reproduce very well the asymmetry of the phase flips in the observed data for Rx053 and Rx054.

SHORT OFFSET PHASE

Short offset phase versus offset (PVO) curves provide useful information for positioning and timing verification. Receivers having a high dynamic range are required in order to acquire these data without signal saturation. The phase of the inline electric field flips when either of the two source electrodes is towed directly above the receiver. Normally, the two flips are symmetric in offset from the receiver position, as seen in Figure 2(top) for receiver Rx052 which resides on a flat region of the seafloor. The asymmetric phase flips that we see for the other two receivers, Rx053 and Rx054, can indicate either problems with the position measurements or that the receiver has moved after the initial positioning.

Note however that the asymmetric data originate from two receivers located on the slopes of a trench. We continue to demonstrate that the observed asymmetry of the PVO curves can be fully attributed to the rough bathymetry , thus restoring confidence in the accurate receiver positioning. For that purpose we have run 3D forward modeling using the bathymetry information from the real survey and a finely gridded model to accurately reproduce the short-offset behavior. The formation resistivity was assumed to be 1.5 Ωm. The computed PVO curves are shown in Figure 3 and demonstrate the same trend as the observed data: PVO is always shifted towards the trench center (for both receivers, Rx053 and Rx054, located on the opposite sides of the trench). This behavior can be understood by considering the direction of field lines close to a dipole source and taking into account the pitch of receivers. Indeed, the same trends have been observed on a number of receivers deployed in trenches in various CSEM surveys. Understanding the connection between the asymmetry of short-offset PVO curves and local bathymetry variations thus helps to qualify data as having good quality.

LONG OFFSET MAGNITUDE

The short offset CSEM data are mostly used for QC and have very little effect on the geological interpretation of the area. The resistivity distribution in the deep subsurface layers is usually recovered using medium and long offset data. Therefore understanding the effect of local bathymetry variations on the long offsets is essential.

Figure 4 shows the bathymetry profile for another survey, also offshore Brazil. Receiver Rx080 is located in the middle of a 2 km long slope in a big trench. Magnitude versus offset (MVO) data for Rx080 and a few neighboring receivers are presented in Figure 5. The data for receiver Rx080 clearly stands out, in particular, the magnitude at the outtow offset of 4 km for Rx080 is 3 times smaller than the magnitude for the neighboring receivers. On the intow the effect is the opposite, but weaker: the signal measured by Rx080 is slightly enhanced.

The very strong deviation between data from Rx080 and neighboring receivers raises several questions: *Should the data from receiver Rx080 be considered an outlier? Can one explain the observed deviation by local bathymetry variations? If yes, does a high sensitivity of data to local bathymetry prevent a reliable geological interpretation?* In order to find the answers to these questions and gain a better understanding of bathymetry effects, we performed a synthetic 3D forward modeling study for a number of receivers located within a trench model.

DOI http://dx.doi.org/10.1190/segam2013-1201.1

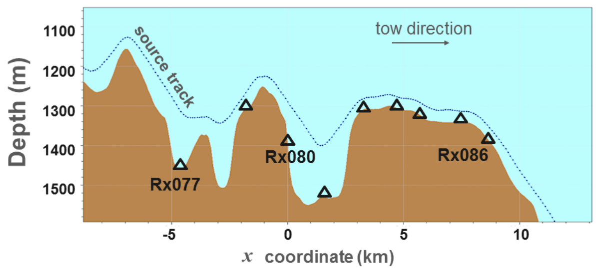

Figure 4: The rough bathymetry profile, receivers (triangles) and CSEM source trajectory from a survey offshore Brazil. Receiver Rx080 is located at the steepest part of the trench slope.

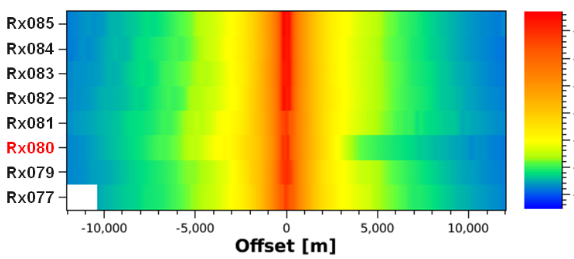

Figure 5: MVO data for the inline electric field E_{in} at 0.12 Hz for several receivers, the color scale indicates $\log|E_{in}|$. Data for Rx080 located on a trench slope (see Figure 4) has anomalously low magnitude on outtow and higher magnitude on intow.

SYNTHETIC TRENCH

We consider the bathymetry depicted in Figure 6, which is flat everywhere except a single trench of an ideal sine-shape, $z = h\sin^2(\pi x/w)$ for $0 \leq x \leq w$. We shall also assume the trench width $w = 600$ m and depth $h = 60$ m, a uniform formation of 2 Ωm, infinite water layer and a horizontal trajectory of the CSEM source with zero pitch. The receiver arms are assumed aligned with the local bathymetry slope, i.e., they measure the inline electric field component directed along the seafloor.

Figure 7 shows the inline field magnitude for a selection of receivers, most of them far away from the trench. The synthetic MVO data for receiver Rx021 located at the steepest part of the trench clearly stand out in the same way as real data for Rx080, Figure 5: the magnitude is strongly reduced on outtow and increased on the intow. It suggests that the anomalous data of receiver Rx080 can be explained by its position on a trench slope. For receiver Rx027 located at the opposite slope of the trench, one can see similar anomalies in the MVO data as for Rx021, only they are mirrowed.

The difference in synthetic MVOs persists to very long offsets, while on the real data it disappears for offsets > 9 km. This is probably because there is only one trench in the synthetic case, but many other bathymetry features in the real survey that start affecting the data at longer offsets. Also note that we did not aim at fitting the observed MVO curves since this would have

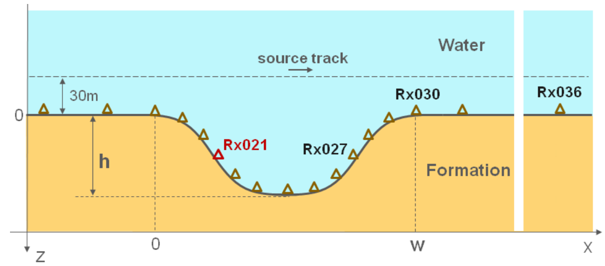

Figure 6: Bathymetry profile, source trajectory and receiver positions used for a synthetic study of the trench effect. Data for receiver Rx021 turned out to be most affected by the presence of the trench.

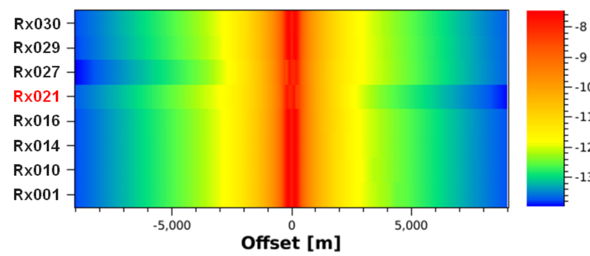

Figure 7: Synthetic MVO data, $\log|E_{in}|$ at 0.1 Hz, computed using the model from Figure 6. Data for receiver Rx021 located on the trench slope shows a strong reduction in the magnitude on outtow and an increase on the intow, as compared to other receivers. These are the same trends as for real data of Rx080 in Figure 5.

required the detailed knowledge of subsurface resistivity. The latter can be obtained by a 3D inversion of the whole dataset, which is currently ongoing.

VARYING TRENCH DIMENSIONS

From the previous section we have understood qualitatively the effect of a seabed trench on MVO data. An open question now is how the observed reduction in the electric field magnitude would depend on the trench width, depth and shape. The ultimate goal would be to find some universal law connecting the trench parameters and the resulting effect on the CSEM data.

For that purpose let us again use the sine-shaped trench of Figure 6. Trenches of widths $w = 600$ and 1800 m and depths h in the range from 48 to 270 m have been modeled, corresponding to various ratios h/w and curvatures $\propto h/w^2$. For each case we evaluated the reduction in the inline electric field magnitude at the outtow offset of 6 km for receiver Rx021 compared to the reference receiver Rx036. The relative reduction is plotted in Figure 8 for two frequencies as a function of the ratio depth-to-width, h/w.

Remarkably, all the data points follow almost the same linear dependence implying that the effect of a trench on CSEM data is mainly determined by a single parameter – the ratio h/w. For example, for $h/w = 0.1$, whether it is a 600 m wide 60 m deep

DOI http://dx.doi.org/10.1190/segam2013-1201.1

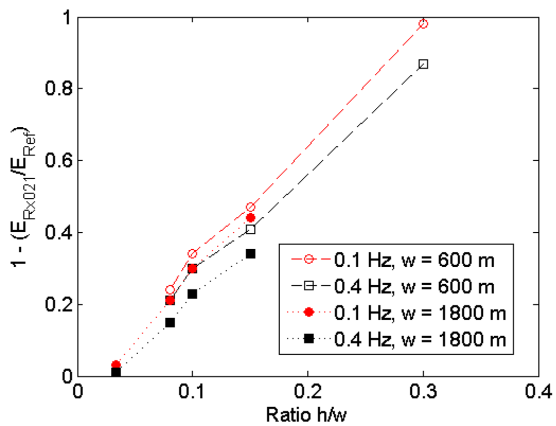

Figure 8: Reduction of the inline electric field for receiver Rx021 on a trench slope compared to a reference receiver, plotted as a function of the trench depth/width ratio.

trench, or a 1800 m wide 180 m deep trench, the reduction in the magnitude for the receiver in the middle of the slope will be approximately the same, 20–30%. There was no uniform data trend when we plotted the same quantity as a function of h, w or h/w^2.

UNCERTAINTY ANALYSIS

Any error in the measured source or receiver position and orientation may be considered as an error in the recorded EM fields. Quantitative analysis of the error propagation for a plane-layered earth with a flat seafloor has recently been performed by Mittet and Morten (2012). If the seafloor is not flat, and has a curvature, then the receiver positioning errors lead to an additional error in the recorded fields compared to that of a flat bathymetry. We shall evaluate this additional bathymetry-induced uncertainty of CSEM data using the synthetic modeling results presented above.

Among the receivers distributed across the trench of Figure 6, we look for the pair of the neighboring receivers where the inline electric fields E_{in} differ the most, i.e., we find the maximum of $|\Delta E_{in}/E_{in}|/|\Delta x_r|$, where $|\Delta x_r|$ is the receiver spacing. For the 600 m wide, 60 m deep trench, 6 km outtow offset and 0.1 Hz this quantity equals to $4 \cdot 10^{-4}\mathrm{m}^{-1}$. Taking a conservative estimate of the receiver positioning error from Table 1, $\delta x_r = 1.5$ m, we then arrive at ≈0.6% error in the recorded inline field. If one approximates the datapoints in Figure 8 by a linear fit, then the folllowing general expression for the uncertainty of the inline electric field can be obtained:

$$\left|\frac{\delta E_{in}}{E_{in}}\right| \approx 24\ \frac{h}{w^2}\ \delta x_r \qquad (1)$$

The squared trench width w in the denominator implies that wide trenches present much smaller challenge for CSEM acquisition. For example, if the width w is as large as 2 km, then even for a 1 km deep trench (having the maximal slope of 57 degrees), the resulting data uncertainty will stay below 1%. Small scale bathymetry features are however less desirable: for $w = 300$ m, the same 1% data uncertainty will be generated by just a 25 m deep trench (with a slope ∼15 degrees).

For a flat seafloor the data uncertainty due to positioning error δx can be very roughly estimated as $|\delta E_{in}/E_{in}| \approx \delta x/\delta_{skin}$ where δ_{skin} is the skin depth. Comparing this to Eq. 1 with $w = 600$ m, frequency 0.4 Hz and resistivity 2 Ωm, we find that the bathymetry-induced uncertainty may dominate the flat-seafloor uncertainty if the trench slope exceeds 4 degrees. This estimate however implies the same positioning error δx in both cases. In case of flat seafloor, positioning errors in both source and receiver contribute to the total δx. As for the bathymetry-induced uncertainty, one can take the source out the picture by choosing a smooth source path well above the bathymetry landscape. Then δx is the positioning error for receivers only, which is known to be much smaller than that for the source electrodes moving through the water (Mittet and Morten, 2012). The presented analysis thus quantifies the benefits of choosing a smooth flight path for the CSEM source: it significantly reduces the data uncertainties and hence ensures the greatest reliability in the final interpretation.

Another contribution to the total data uncertainty comes from inaccurate knowledge of the bathymetry landscape itself. If it is provided on a coarse grid only, the corresponding data uncertainty can dominate over that related to receiver positioning errors. Finally, we emphasize that the quantitative results presented here apply only to the considered sine-shaped trench, but we do not see any reasons why our conclusions should not hold also for other realizations of rough bathymetry.

CONCLUSIONS

We have analyzed the effects of rough bathymetry on the reliability of the marine CSEM method in synthetic and real data. For a receiver deployed at the intow slope of a trench we show that its short offset phase curve shifts in the outtow direction, while the magnitude of inline eletric field is strongly reduced for the outtow offsets. Understanding these trends is essential for proper data QC. The key trench parameter that determines how much the recorded inline field is affected, is shown to be the depth-to-width ratio. We evaluate the uncertainty in the CSEM data caused by rough bathymetry and show that high positioning accuracy is important when the seafloor slope variations occur over short distances. It is demonstrated that the observed bathymetry effects on the data can be modeled if the bathymetry information is available, and thus allows for reliable inversion of the data. Finally, we explain why smoothed source flight paths significantly increase the reliability of marine CSEM data in the presence of rough bathymetry.

ACKNOWLEDGMENTS

The authors wish to thank EMGS for permission to publish the results as well as F. Roth, J. Tinder, D. Ridyard and T. Bratteland for valuable comments.

DOI http://dx.doi.org/10.1190/segam2013-1201.1

http://dx.doi.org/10.1190/segam2013-1201.1

EDITED REFERENCES

Note: This reference list is a copy-edited version of the reference list submitted by the author. Reference lists for the 2013 SEG Technical Program Expanded Abstracts have been copy edited so that references provided with the online metadata for each paper will achieve a high degree of linking to cited sources that appear on the Web.

REFERENCES

Constable, S., 2010, Ten years of marine CSEM for hydrocarbon exploration: Geophysics, **75**, no. 5, 75A67–75A81.

Eidesmo, T., S. Ellingsrud, L. MacGregor, S. Constable, M. Sinha, S. Johansen, F. Kong, and H. Westerdahl, 2002, Sea bed logging (SBL), a new method for remote and direct identification of hydrocarbon-filled layers in deepwater areas: First Break, **20**, 144–152.

Mittet, R., and J. P. Morten, 2012, Detection and imaging sensitivity of the marine CSEM method: Geophysics, **77**, no. 6, E411–E425, http://dx.doi.org/10.1190/geo2012-0016.1.